Research Article

Alexander Brodsky and Natan Kaplan*

M^6 formalism – generalization of the laser beam quality factor M^2 to the 3D domain

https://doi.org/10.1515/aot-2020-0007
Received March 5, 2020; accepted April 6, 2020

Abstract: Here we define a theoretical basis for the generalization of the beam quality factor M^2 to three-dimensional (3D) space, which we call M^6 formalism. The formalism is established through the use of examples of multifocal and Axicon optical systems to illustrate discrete and continuous axial beam shaping, respectively. For the continuous case, we expand the definition of the Rayleigh range to incorporate a quality factor having both axial and transverse components M^2_{add} and M^2. Using geometrical ray tracing simulations, a proportion factor C is found to empirically describe the axial quality factor M^2_z of an optical setup including an Axicon and a paraxial focusing lens with a Gaussian single mode input beam. Using our M^6 formalism depth of focus (DOF) ranges are calculated for higher M^2 beams, and are shown to be in good agreement with the simulated DOF range, demonstrating the usefulness of the M^6 formalism for the design of real optical systems.

Keywords: beam parameter product; beam shaping; Bessel-like beam; coherence; diffractive multifocal lens; laser beam quality; M^2; multimode laser; optical entropy; Rayleigh range.

1 Introduction

In recent years there are an increasing number of scientific and industrial applications requiring laser beam manipulation along the optical axis. For research these are, for example, light-sheet microscopy [1, 2], optical trapping (tweezers) [3, 4], cytometry [5], and stimulated emission depletion (STED) [6], while an example of industrial applications is laser glass cutting [7, 8]. Many examples of three-dimensional (3D) spatial coherence were recently reviewed by Flamm and his colleagues in their review article for 3D beam shaping [9]. Commonly used on-axis (Z axis) shapes in these applications are Bessel-like beams and multiple foci beams, but there is no convenient way to describe the characteristics of such beams, and usually they are described in terms of the generating optic. Thus, there is a need in the laser industry to define common convenient rules to describe beam characteristics, for cases where the Z axis is involved. Here, we will expand the standard transverse model for laser beam quality factor M^2 by adding another dimension that is the propagation axis of the light.

2 Analytical formulation of M^6 formalism

The beam quality factor (M^2) for transverse beams has been widely investigated in the scientific literature, and was developed by Siegman [10, 11] c. 1998. The concept of laser beam quality is based on aggregating the statistics of beams with arbitrary profiles to predict their size and divergence in different planes along the propagation path. To state this simply – the M^2 factor describes 'how far' a real beam is from the base mode of an ideal Gaussian beam with an M^2 equal to 1. Certain families of multimode beams such Gauss-Hermite with Cartesian symmetry M^2_x and M^2_y or Gauss-Laguerre with polar symmetry M^2_R and M^2_θ have separated orthogonal values for M^2 for each axis and their M^2 has an analytical expression [12]. Another widely known family of the multimode beams is arbitrary (not analytical), such as the output intensity from multimode fibers [13], laser diodes, vertical-cavity surface-emitting laser (VCSEL) single emitters and arrays and others. The overall beam quality of transverse beams M^4 is defined as a two-dimensional (2D) integral of the divergence angle and intensity at any point over the entire beam area [14].

***Corresponding author: Natan Kaplan,** Holo/Or LTD, R&D, Ness Ziona, Israel, e-mail: natan@holoor.co.il. https://orcid.org/0000-0003-1500-3186
Alexander Brodsky: Holo/Or, Ness Ziona, Israel. https://orcid.org/0000-0001-7770-9999

www.degruyter.com/aot

© 2020 THOSS Media and De Gruyter

Published online May 16, 2020

For a better understanding we can consider that M^2 is similar to the term of statistical entropy that describes the level of disorder in 3D space, in our case, of optical complex fields consisting of amplitude and phase. By analogy we can assume the existence of M^2 in the Z (light propagation) axis. As a consequence, the overall beam quality factor in Cartesian coordinates is defined by $M^6(M_x^2, M_y^2, M_z^2)$. It is important to note that M_z^2 is a purely spatial coherence property and it does not refer to the temporal coherence of the laser.

The M^6 formalism of laser beams can simplify understanding of the so-called 'non-diffractive' [15], or 'self-healing' [16, 17] phenomena referring, for example, to Bessel-like beams [18, 19] and Airy beams [20]. Those beams are a special kind of multimode beam, with a strong effect of M_z^2 on their behavior.

For commonly used continuous planar and spherical optical elements, including prisms, spherical lenses, planar, and focusing mirrors, this M_z^2 has no meaning. Any near and far field (waist point) planes using this group of elements keep the beam quality factor constant and can be described by transverse coordinates only. This is a possible explanation as to why this issue of M_z^2 was not investigated previously.

The phenomenon of M_z^2 is revealed when utilizing optical elements that change the behavior of the laser beam along the optical axis. For example, different types of Axicons that create a Bessel-like beam region called the extended depth of focus (DOF) region [21, 22], and diffractive multifocal lenses that split an incident beam into discrete diffraction orders along the optical axis [23, 24].

3 Examples of M^6 and M_z^2

3.1 Multifocal lens – discrete axial shaping

We will use the multifocal lens as the first example to demonstrate the existence of the M_z^2 phenomenon. Let us consider an ideal multifocal diffractive lens with five foci. The diffractive lens foci positions are expressed by the following equation:

$$f_m = \frac{f_1}{m} \tag{1}$$

where f_m is focal length of m diffraction order, and f_1 is focal length of diffraction order 1. In analogy with diffraction gratings, all diffraction orders have the same optical properties as the incident beam, but individual directions defined by the grating equation. Each axial order (focus) is an exact copy of the parent incident beam, with an individual combination of spot size and beam divergence. Each order can be considered as a virtual light source with a waist in position f_m. This conceptual comparison of multifocal diffraction lens and diffraction gratings is described in Figure 1. Figure 1 (left) shows five Gaussian waists arranged along the X axis with M^2 per axis as follow $M_x^2 = 5$ (sum of all in the X axis), and $M_y^2 = M_z^2 = 1$. Such emitters arrangement exists for example in VCSEL arrays [25]. Figure 1 (right) shows the multifocal case of five Gaussian emitters placed along Z axis and $M_x^2 = M_y^2 = 1, M_z^2 = 5$ (sum of all in the Z axis). For both cases overall beam quality factor in 3D space is identical and equal to $M^6 = M_z^2 \cdot M_x^2 \cdot M_y^2 = 5$.

From this example, we see that calculation of M_z^2 in a case of multifocal lens is very simple and expressed by M_z^2 sum of all foci:

$$M_{z\_\text{total}}^2 = N \cdot M_z^2 \tag{2}$$

where N is number of foci and M_z^2 is axial beam quality factor of individual focus. M_z^2 for a multifocal lens equal to 1, as each focus is the same as a focus of a separate single lens, which as we know does not have an axial shaping effect, unlike the case for a Bessel-like beam which we will discuss now.

3.2 Axicon – continuous axial shaping

As the second example of axial laser beam quality factor effect, we will consider an Axicon element. An Axicon is

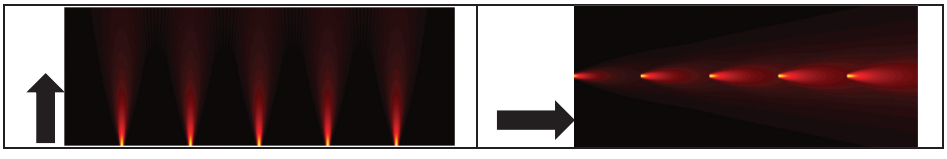

Figure 1: Left image demonstrates example of well-known arrangement of single mode sources along X axis. Right image shows same sources arranged along Z axis. Overall beam quality along the X and Z axes, respectively, is a sum of all individual sources, identical for both cases.

also called a radial prism or radial grating. For the multifocal lens example, we had N foci referring to N discrete geometrical focal points, for an Axicon we take this N to infinity, to a continuity of focal segments, each having the same NA. On Figure 2 left we see a 2D layout of geometrical rays for an ideal trifocal lens. Each focus is, colored individually. The blue, green, and red line color refers to diffraction orders 1, 2, and 3, respectively. Each focus has different NA. Figure 2 right shows rays' distribution after an ideal Axicon, all focal regions have the same NA.

3.2.1 Generalization of Rayleigh range to M^6 formalism

The Rayleigh range is used to determine the DOF in conventional optics, thus, we will need to generalize it for cases with axial shaping. As a mathematical basis to generalize the Rayleigh range definition so that it fits the M^6 formalism, we will start from the known set of definitions for waist spot size and Rayleigh range shown in Table 1.

In this model the Rayleigh range, which describes beam behavior along the optical axis, is not a function of the z coordinate. Then, by analogy with spatial factor of M^2 for spot size, we multiply the Rayleigh range by a new parameter M_z^2 – the beam quality factor in Z axis. This new parameter includes two components related to axial behavior: the already familiar transverse M^2, and a new component related to independent axial beam quality factor M_{add}^2. Combining of the two components is done by using a root mean square (RMS) value [26, 27]. The generalized formula for Rayleigh range with beam quality factor in Z axis becomes:

$$Z_R = M_z^2 Z_{R0} = \sqrt{(M_{\text{add}}^2)^2 + (\mathrm{M}^2)^2} \cdot Z_{R0} \tag{3}$$

where M_{add}^2 is the axial beam quality factor, M^2 is the transverse (traditional) beam quality factor, Z_R is the new Rayleigh range, and Z_{R0} is the single mode beam Rayleigh range.

From eq. (3), we see that the generalized Rayleigh range is determined by two independent parameters – the axial and transverse quality factors. When focusing a beam where the axial beam quality factor M_{add}^2 is high, while the transverse quality factor M^2 is low, one obtains a useful combination of a tightly focused central spot and a long depth of focus.

In the multifocal lens example, we saw that M_z^2 was proportional to the number of foci. The method to calculate the M_z^2 of a Bessel-like beam generated by an Axicon is to measure how many times the transverse Rayleigh range is contained in the Bessel region. We will show this on a typical setup with an ideal positive (convex) type Axicon and ideal focusing lens shown in Figure 3 (left). The Axicon generates two regions of interest here – a Bessel-like beam region (DOF) and an annular or ring-shaped beam region in focal plane F of the lens. In our example the incident beam is collimated and therefore the focal plane is the same as the focal plane of the ideal lens.

Before finding the final expression to describe the DOF of an Axicon element, we should take the effect of the shifting 'waist' position of the DOF region into account. The new F' focal length, defined as the position along the optical axis that has the peak intensity, is calculated geometrically from the sum of Axicon ring angle β and the NA of the Gaussian laser beam angle θ and shown in eq. (4). For convex Axicons the ring angle has a positive sign and vice versa for concave Axicons. Schematically, rays' directions are shown in Figure 3 (right).

$$F' = \frac{d}{2\tan(\theta + \beta/2)}; \theta = \tan^{-1}\left(\frac{d}{2F}\right) \tag{4}$$

We know that the Axicon's DOF is affected by the Axicon's ring angle β, as defined in Figure 3 (right) as the angle between the rays after the Axicon. Therefore, we will assume that M_{add}^2 is directly proportional to the Axicon's ring angle, and inversely proportional to beam size.

Next, we define M_{add}^2 as the ratio of the natural divergence of a single mode Gaussian input beam φ_{0_input} with diameter d to the ring angle of the Axicon β:

$$\varphi_{0\_\text{input}} = \frac{4\lambda}{\pi d}; M_{\text{add}}^2 = \mathrm{C} \cdot \frac{\beta}{\varphi_{0_{\text{input}}}} = \mathrm{C} \cdot \frac{\pi \cdot d \cdot \beta}{4 \cdot \lambda} \tag{5}$$

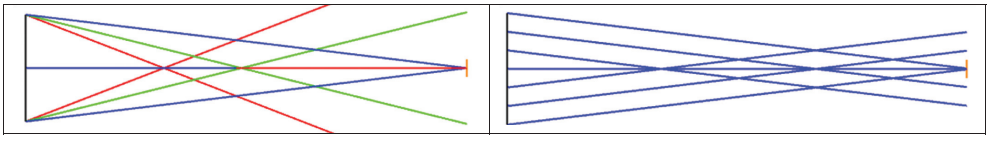

Figure 2: 2D layout with geometrical rays. Left: ideal diffractive multifocal lens with individual colour for each focus. Each focus has different NA value. Right, ideal positive Axicon. All rays have same NA.

Table 1: Diffraction limited spot size and Rayleigh range, for multimode and single mode beams.

	Single mode beam	Multimode beam
Spot size in focal plane	$\omega_0 = \frac{4\lambda F}{\pi d}$	$\omega_{MM} = M^2 \frac{4\lambda F}{\pi d}$
Rayleigh range	$Z_{R0} = \frac{\pi\omega_0^2}{\lambda} = \frac{4\lambda}{\pi}\left(\frac{F}{d}\right)^2$	$Z_{R\_MM} = \frac{\pi\omega_{MM}^2}{\lambda} = M^2 \frac{4\lambda}{\pi}\left(\frac{F}{d}\right)^2$

Where λ is the wavelength, d is the input beam diameter at exp(−2), and F is the focal length of the lens.

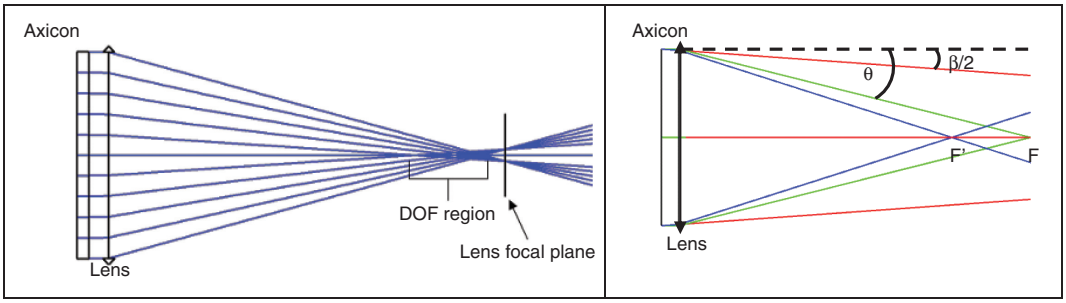

Figure 3: Left, 2D layout of an Axicon and lens optical system with geometrical rays. The setup includes an ideal positive Axicon element, and an ideal focusing lens. The DOF region occurs before the focal plane, and the annular beam is in the focal plane. Right, geometric presentation of optical marginal rays of an optical setup from the Left. Red color lines refer to the Axicon's ring angle β, green lines refer to the NA of the Gaussian laser beam angle θ rays that intersect in the focal plane F, and blue colored lines refers to the sum of focusing and ring angles intersect in focal plane F'. F' is a new position with maximum on axis intensity.

In eq. (5) we define the C factor as the proportion factor responsible for DOF in the single mode input case. We will find the C factor empirically in the next section.

After finding F', the location of the position with peak intensity along Z axis, we define the depth of focus Δ_p as the distance from F' required for the intensity to drop to $p \cdot I(F')$. Our generalized form of the depth of focus equation (detailed derivation shown in the Appendix) for a real beam in a medium with a refractive index n has the following form:

$$\Delta_p = n \cdot \sqrt{(M_{add}^2)^2 + (M^2)^2} \cdot 2Z_{R0}\sqrt{\frac{1}{1-p} - 1} \quad (6)$$

where M_{add}^2 is given by (5), M^2 is the transverse (traditional) quality factor and Z_{R0} is the Rayleigh range for a single mode beam with the same diameter. For the particular case of the intensity drop $p = 0.5$, the depth of focus equation of an Axicon becomes equal to twice the generalized Rayleigh range from (3):

$$\Delta_{Axicon_{0.5}} = n \cdot M_z^2 \cdot 2 \cdot Z'_{R0} = n \cdot \sqrt{(M_{add}^2)^2 + (M^2)^2} \cdot \frac{8\lambda}{\pi}\left(\frac{F'}{d}\right)^2; \quad (7)$$

In the next section we find the proportion factor C from (5) (necessary to calculate M_{add}^2) using simulations of an Axicon along the Z axis.

3.2.2 Determination of the constant C for the Axicon and lens optical setup by simulation

To calculate the C constant, we use a geometrical Raytracing simulation to calculate the DOF for a variety of M^2 values (1–5), with the M^2 values are defines using a scattering model as described in the reference [28].

The geometric optics raytracing simulations were done in Zemax™ (LLC, Kirkland, WA, USA) OpticStudio, for a wavelength of 1064 nm, with input defines as a Gaussian beam with diameter of 6 mm at exp(–2). This beam passes through an Axicon with a ring angle of 1.129 mRad (defined using a radial diffraction grating) and then is the focus by an ideal focusing lens with an effective focal length (EFL) of 20 mm.

In Figure 4 we show the axial intensity distribution of a Bessel-like beam generated by an Axicon around the F' position with an incident beam having varying quality factors from 1 to 5. Rulers were added at 50% of the F' peak intensity to show the DOF values.

The calculations below (Table 2) were used to find the empirical value of the C factor from (5).

Calculations are in good agreement (<4% difference) with the simulated DOF length for a single mode beam and using the derived $C_{0.5}$ for higher M^2 beams gave DOF values that were also in good agreement with the simulations (see Figure 4).

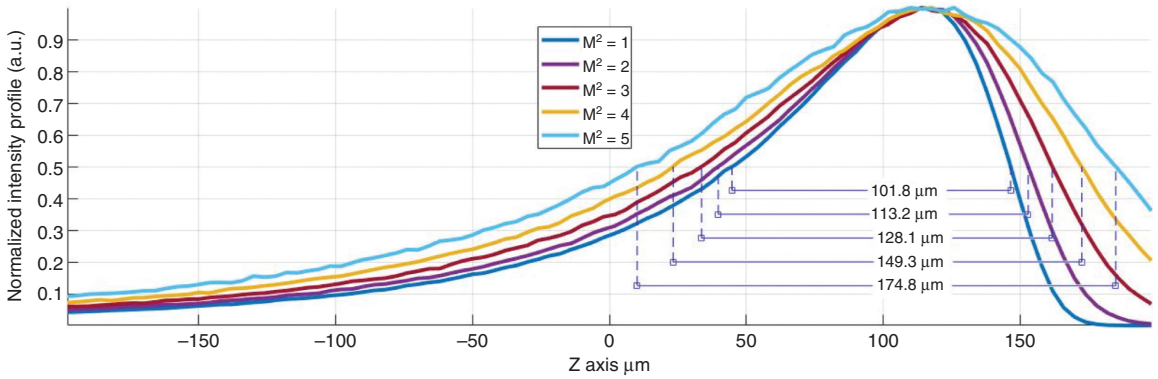

Figure 4: Intensity profile along the Z axis for a Bessel-like beam generated by an Axicon with incident beams having M^2 from 1 to 5.

Table 2: Calculation of DOF and $C_{0.5}$ constant for an axicon and focus lens setup, for input beams with M^2 from 1 (single mode) to 5.

The new focal position F due to shifting by the Axicon	$F' = \frac{d}{2\tan\left(\tan^{-1}\left(\frac{d}{2F}\right)+\beta/2\right)} = \frac{6}{2\tan\left(\tan^{-1}\left(\frac{6\,\text{mm}}{2\cdot 20\,\text{mm}}\right)+\frac{1.129E-3}{2}\right)} = 19.923\,\text{mm}$
Rayleigh length for single mode	$Z_{R0} = \frac{4\lambda}{\pi}\left(\frac{F}{d}\right)^2 = \frac{4\cdot 1.064\,\mu\text{m}}{\pi}\left(\frac{20\,\text{mm}}{6\,\text{mm}}\right)^2 = 15.1\,\mu\text{m}$
Shifted Rayleigh length	$Z'_{R0} = \frac{4\lambda}{\pi}\left(\frac{F'}{d}\right)^2 = \frac{4\cdot 1.0644\,\mu\text{m}}{\pi}\left(\frac{19.923\,\text{mm}}{6\,\text{mm}}\right)^2 = 14.9\,\mu\text{m}$
DOF for Gaussian	$\Delta_{\text{Gaussian\_0.5}} = 2Z_{R0} = 30.2\,[\mu\text{m}]$
DOF for Bessel-like beam, M^2_{add}, and M^2_z for Gaussian input	$\Delta_{\text{Axicon}_{0.5}} = 2\sqrt{(M^2_{\text{add}})^2+(M^2)^2}\cdot Z'_{R0} = 2\cdot\sqrt{(M^2_{\text{add}})^2+1}\cdot 14.94\,\mu\text{m} = 101.8\,\mu\text{m}$ $M^2_{\text{add}} = 3.2665;\quad M^2_z = \sqrt{3.2665^2+1} = 3.416$
Constant C	$M^2_{\text{add}} = C_{0.5}\cdot\frac{\pi\cdot\theta\cdot d}{4\cdot\lambda} = C_{0.5}\cdot\frac{\pi\cdot 1.129\,\text{mrad}\cdot 6\,\text{mm}}{4\cdot 1.064E-3\,\text{mm}} = 3.2665$ $C_{0.5} = 0.6533$
DOF for higher M^2 of incident beam	$\Delta_{\text{Axicon}_{0.5}} = 2\cdot\sqrt{3.2665^2+(M^2_i)^2}\cdot 14.9,\ \text{where } M^2_{i=[1,2,..5]} = 1,2,3,4,5$ $\Delta_{\text{Axicon}_{0.5}} = 101.8, 114.1, 132.2, 153.9, 178.0\,\mu\text{m}$

DOF, depth of field.

4 Calculation and measurement of M_z^2

M^2 of ideal multimode lasers like Gauss-Hermite or Gauss-Laguerre have analytical solution. M^2 calculation of real, arbitrary beams is not a trivial task, for both real measurement, and simulations. Existing instruments used to measure the beam quality factor can measure the transverse beam quality of continuous beams in optical systems composed only of elements without axial shaping effects. The future devices for measurement of M^6 and M_z^2 will have to consider the existence of these axial phenomena and to include mathematical algorithms for dedicated analysis.

Simulation tools with physical optics capabilities are also limited by the same conditions [29]. Some certain examples of M^2 can be calculated from knowledge about the system. For example, fiber core and NA define the maximum M^2 of the output [30], divergence angle of a diffuser and beam size allow a good estimation for M^2, number of emitters in array or diffraction orders configuration for periodic diffraction optical elements (DOEs).

Calculation of the M⁶ beam quality from M_z^2 term is not trivial without preliminary knowledge about the system; i.e. what kinds of optical elements are used and their geometry.

5 Summary and discussion

The M⁶ beam quality factor formalism of volume spatial coherence in optics expands the well-known transverse model of beam quality to 3D space. In this model there is an additional spatial coherence quantity spread along the light propagation direction. The generalized 3D laser illumination quality factor M⁶ is represented by the quality parameters M_x^2, M_y^2, M_z^2. For continuous shaping, the M_z^2 is an additional factor multiplier of the standard Rayleigh range in the Gaussian optics formulas. M_z^2 for a Bessel-like beam output of an Axicon was simulated and a mathematical expression for DOF length in a basic optical setup was empirically found, allowing one to calculate the DOF for any combination of system parameters (focus lens EFL, input beam quality, input beam diameter and axicon angle β).

M⁶ formalism opens new opportunities in the field of 3D beam shaping and coherence manipulations. Examples of fields where this formalism can be of use include laser systems for spatial transformation from transverse axes to longitudinal or vice versa, waveguides combined with diffraction grating in augmented reality devices, multimode fiber systems [31], fiber coupling [32–34], laser cavities with special geometry [35, 36], crystal pumping [37] and more.

There are no ready commercially available simulation and measurement tools for M⁶ as of the time of this article's publication. We hope that new applications that utilize the 3D beam quality will encourage the development of such tools.

6 Appendix

6.1 Generalized DOF formula

The generalized DOF formula is derived from the well-known Gaussian waist size equation:

$$\omega_z = \omega_0 \sqrt{1+\left(\frac{Z}{Z_R}\right)^2} \tag{8}$$

where ω_z, and ω_0 are beam sizes in distance Z from focal plane.

We define p factor as the intensity drop from its maximum in the focal plane, and it is proportional to the beam squared beam size (area).

$$p = 1-\frac{\omega_0^2}{\omega_z^2}, \frac{\omega_0^2}{\omega_z^2} = 1-p \tag{9}$$

Expressing Z from (8)

$$Z^2 = Z_R^2\left(\frac{\omega_z^2}{\omega_0^2}-1\right) \tag{10}$$

Substituting p in (9)–(10)

$$Z^2 = z_R^2\left(\frac{1}{1-p}-1\right) \tag{11}$$

Z is only half DOF range Δ_p, and it is proportional to refractive index n.

Using (3) the final expression for DOF is:

$$\Delta_p = \mathrm{n}\cdot\sqrt{M_{\mathrm{add}}^2+\mathrm{M}^2}\cdot 2Z_{R0}\sqrt{\frac{1}{1-p}-1} \tag{12}$$

References

[1] L. Gao, L. Shao, B.-C. Chen and E. Betzig, Nat. Protoc. 9, 1083 (2014).
[2] F. O. Fahrbach, V. Gurchenkov, K. Alessandri, P. Nassoy and A. Rohrbach, Opt. Express 21, 13824–13839 (2013).
[3] J. Arlt, V. Garcés-Chávez, W. Sibbett and K. Dholakia, Opt. Commun. 197, 239–245 (2001).
[4] Y. Zhang, X. Tang, Y. Zhang, W. Su, Z. Liu, et al., Opt. Lett. 43, 2784–2786 (2018).
[5] B. B. Collier, S. Awasthi, D. K. Lieu and J. W. Chan, Sci. Rep. 5, 10751 (2015).
[6] P. Zhang, P. M. Goodwin and J. H. Werner, Opt. Express 22, 12398–12409 (2014).
[7] K. Mishchik, R. Beuton, O. Dematteo Caulier, S. Skupin, B. Chimier, et al., Opt. Express 25, 33271–33282 (2017).
[8] R. Stoian, M. Bhuyan, G. Zhang, G. Cheng, R. Meyer, et al., Adv. Opt. Technol. 7, 165–174 (2018).
[9] D. Flamm, D. G. Grossmann, M. Jenne, F. Zimmermann, J. Kleiner, et al., in 'Laser Resonators, Microresonators, and Beam Control XXI (Vol. 10904, p. 109041G)' (International Society for Optics and Photonics, 2019).
[10] A. E. Siegman, Diode Pumped Solid State Lasers: Applications and Issues (Optical Society of America, 1998).
[11] J. Alda, Encyclopedia Opt. Eng. 2013, 999–1013 (2003).
[12] S. Saghafi, C. J. R. Sheppard, Opt. Commun. 153, 207–210 (1998).
[13] R. Paschotta, Beam Quality Limit for Multimode Fibers. in the RP Photonics Encyclopedia (accessed on 2019-06-09).

[14] N. Davidson and B. Nandor, Prog. Opt. 45, 1–52 (2003).
[15] J. Durnin, J. Miceli Jr and J. Eberly, Phys. Rev. Lett. 58, 1499 (1987).
[16] D. McGloin and K. Dholakia, Physics 46, 15–28 (2005).
[17] V. Jarutis, R. Paškauskas and A. Stabinis, Opt. Commun. 184, 105–112 (2000).
[18] R. Borghi and M. Santarsiero, Opt. Lett. 22, 262–264 (1997).
[19] R. M. Herman and T. A. Wiggins, Appl. Opt. 37, 3398–3400 (1998).
[20] R. P. Chen, et al., Opt. Laser Technol. 44, 2015–2019 (2012).
[21] K. S. Lee and P. R. Jannick, Opt. Lett. 33, 1696–1698 (2008).
[22] R. A. Leitgeb, M. Villiger, A. H. Bachmann, L. Steinmann and T. Lasser, Opt. Lett. 31, 2450–2452 (2006).
[23] Y. G. Soskind, Field Guide to Diffractive Optics (SPIE, Bellingham, WA, 2011).
[24] D. C. O'Shea, T. J. Suleski, A. D. Kathman and D. W. Prather, Diffractive Optics: Design, Fabrication, and Test (Spie Press, Bellingham, WA, 2004) Vol. 62.
[25] K. A. Ingold, et al., CLEO: Applications and Technology (Optical Society of America, 2018).
[26] N. Trela, Spatial and Spectral Brightness Improvement of Single-Mode Laser Diode Arrays. Diss (Heriot-Watt University, 2012).
[27] P. Loosen and K. Alexander, Incoherent Beam Superposition and Stacking. in 'High Power Diode Lasers' (Springer, New York, NY, 2007) pp. 121–179.
[28] A. Brodsky and N. Kaplan, Method for Laser Source Definition in ZEMAX. https://www.holoor.co.il/wp-content/uploads/2019/12/Method-For-Laser-Source-Definition-in-ZEMAX-To-Enable-Realistic-Modelling-With-Raytracing.pdf?x52531.
[29] D. M. Hasenauer and D. S. Bryan, 'Optical Systems Design 2015: Optical Design and Engineering VI. Vol. 9626' (International Society for Optics and Photonics, 2015).
[30] R. Paschotta, Optical Heterodyne Detection. in 'The RP Photonics Encyclopedia' (accessed on 2019-04-27).
[31] S. R. Lee, J. Kim, S. Lee, Y. Jung, J. K. Kim, et al., Opt. Express 18, 25299–25305 (2010).
[32] H. Melkonyan, K. Sloyan, K. Twayana, P. Moreira and M. S. Dahlem, IEEE Photonics J. 9, 1–9 (2017).
[33] P. Markov, G. V. Jason and M. W. Sharon, Opt. Express 20, 14705–14713 (2012).
[34] H. Kuwahara, M. Sasaki and N. Tokoyo, Appl. Opt. 19, 2578–2583 (1980).
[35] F. Wu, C. Yunbin and G. Dongdong, Appl. Opt. 46, 4943–4947 (2007).
[36] A. Khilo, G. K. N. Eugeny and A. R. Anatol, JOSA A 18, 1986–1992 (2001).
[37] V. Pasiskevicius, H. Karlsson, J. A. Tellefsen, F. Laurell, R. Butkus, et al., Opt. Lett. 25, 969–971 (2000).